



# Hydrogen evolution assisted cyclic electroplating for lateral copper growth in wearable electronics



Sabrina M. Rosa-Ortiz, Kat-Kim Phan, Nida Khattak, Sylvia W. Thomas, Arash Takshi\*

Department of Electrical Engineering, University of South Florida, Tampa, FL 33620, USA

## ARTICLE INFO

### Keywords:

Electrodeposition  
Lateral growth  
Copper nanostructure  
Hydrogen evolution assisted (HEA)  
electroplating

## ABSTRACT

Recent progress in hydrogen evolution assisted (HEA) electroplating has shown promises for fast lateral growth of copper on various rigid and flexible substrates. In this method, concurrent to the copper reduction, hydrogen bubbles are generated at the cathode resulting in a porous copper layer with a growth rate a few orders of magnitude faster than the standard electroplating method. However, the application of constant voltage does not allow bubbles to leave the surface resulting in non-uniform copper growth and unpredictable nanostructures. To allow the hydrogen bubbles to leave the surface, we have applied a cyclic electroplating method in a voltage range that the electroplating alternates between the HEA and non-HEA modes. The effect of the voltage range and the voltage scan rate on the lateral growth of copper and the quality of the copper layer were investigated on a patterned copper track on a standard printed circuit board (PCB). The fastest growth rate of 55  $\mu\text{m/s}$  was obtained for a voltage range between  $-1.5\text{ V}$  and  $-0.8\text{ V}$  with a scan rate of 100 mV/s. The scanning electron microscopy (SEM) images of different samples revealed that the scan rate affects the nanostructure of the grown copper layer. The feasibility of applying the HEA cyclic electroplating method for developing wearable electronics was demonstrated by growing copper on a piece of fabric to make contact with the pins of a light emitting diode.

## 1. Introduction

The electrodeposition process was introduced more than a century ago as a manufacturing technique where an anode was used to ensure passage of current through the electroplating cell for the deposition [1]. With the development in electronic devices, Cu electrodeposition has been used widely for fabricating printed circuit boards (PCBs) and many other electronic components [2,3]. Electrodeposition of metals is the most cost-effective way to achieve deposition commonly used in the electronics manufacturing industry [4,5]. Also, electrodeposition has been used for the metallization of conductive substrates to improve their conductivity [6].

In conventional copper electroplating, using an electrochemical cell, a few hundred millivolts are applied between a copper counter electrode (anode) and the working electrode (cathode) [7]. The passage of current through the cell forces the movement of ions. In general, the motion of ions in the electrolyte is governed by diffusion, migration, and convection [8]. Once the ions are near the working electrode, the migration and convection are negligible, and the growth rate of the copper is dominated by the diffusion of ions from the bulk

solution towards the surface of the working electrode. The growth rate and quality of the deposition are both affected by the speed at which copper ions reach the cathode [4]. The restriction imposed by the ions mass transfer in the cell usually results in a slow copper growth in a galvanostatic or potentiostatic deposition mode (i.e., constant current or voltage) [8]. To enhance the deposition rate, a large overpotential can be applied across the cell. However, as we have shown in our previous work, the application of a constant DC voltage higher than 1.23 V leads to the release of hydrogen bubbles at the working electrodes producing a porous structure of copper [9,10]. This method of electroplating is known as hydrogen evolution assisted (HEA) electrodeposition. The consequence of the concurrent reduction of  $\text{Cu}^{2+}$  and  $\text{H}^+$  at the cathode is an incredible speed of growth due to the convection of copper ions and more importantly formation of a porous copper layer instead of a compact deposition [11–14]. In our earlier works, we have studied the effect of the concentration of the electrolyte and the applied DC voltage on the speed and the quality of the HEA-grown copper [9,10,15]. A lateral growth speed as high as 15.6  $\mu\text{m/s}$  was obtained when a constant voltage of 1.3 V was applied between the anode and the cathode during the growth [10]. However,

\* Corresponding author.

E-mail address: [atakshi@usf.edu](mailto:atakshi@usf.edu) (A. Takshi).

the main challenge in applying a constant voltage is that there is no control of the hydrogen bubbles being released and interacting with the surface of the working electrode [16]. The constant interaction of the hydrogen bubbles restricts the complete deposition of copper which also creates a limitation at the electrode-electrolyte interface for an effective charge transfer to the cations, ultimately stopping the deposition.

As a solution to this restriction and to produce a more uniform and predictable nanostructure, instead of a constant voltage, in this work, we have applied the cyclic electroplating method around 1.23 V. By alternating the voltage above and below 1.23 V, in a portion of each cycle when the hydrogen evolution occurred, a high growth rate was achieved. The rest of each cycle gave time for the generated bubbles to leave the surface. We have studied the effect of the scan rate and the voltage range on the lateral growth speed and the quality of the deposited layer. Then the HEA cyclic electroplating method was applied to make a copper pattern on a piece of fabric and grow copper to “solder” a light emitting diode (LED) to the copper track on the fabric.

## 2. Materials and methods

The working electrodes with a gap of 1 mm were made by etching FR-4 PCB boards in a ferric chloride etching solution. The pattern was applied using a permanent marker. After etching, the electrodes were immersed in acetone for 1 min to remove the permanent marker ink. Then, it was washed with water to remove any residue left. The samples were properly dried and polished with sandpaper to remove any marks over the surface. Two pieces of wires were soldered to the copper pads for easy connection to the potentiostat instrument.

A piece of copper wire with diameter measures of 0.23 cm was used throughout the work as the anode electrode and 2 mL of an electrolyte made of  $\text{CuSO}_4$  (0.47 M) and  $\text{H}_2\text{SO}_4$  (1.5 M) in deionized water was used with the electrodes to assemble the electrochemical cell. To properly hold the electrolyte, an O-ring of 2.54 cm in diameter was placed between the two pieces of plexiglass that completed the cell (Fig. 1a).

The copper growth was conducted using the cyclic voltammetry (CV) method between a  $V_{\min}$  and a  $V_{\max}$  at different scan rates of 5, 10, 20, 50, 100, 300, and 500 mV/s using VersaStat 4.0 potentiostat in a two-electrode configuration at room temperature while both working electrodes were connected together (Fig. 1.a). In this work,

four different voltage ranges were studied: a)  $-1.3 \text{ V} \leq V \leq -0.8 \text{ V}$ , b)  $-1.5 \text{ V} \leq V \leq -0.8 \text{ V}$ , c)  $-1.3 \text{ V} \leq V \leq -1.0 \text{ V}$ , and d)  $-1.5 \text{ V} \leq V \leq -1.0 \text{ V}$ . It should be noted that although the three-electrode configuration is a common method for studying the working electrodes in electrochemical cells, as the ultimate objective of this project is to design a copper printing machine in future, we conducted the experiments in a two-electrode configuration to find the most suitable voltage range and scan rate for the printer to be designed.

The lateral growth was monitored by video recording the electroplating process using a digital microscope. The lateral growth rate was estimated through the recorded videos by measuring the time that it took for the copper to grow across the 1 mm gap. The surface morphology was observed by a Quanta 200 3D Dual Beam scanning electron microscope (SEM). Although during the HEA water electrolyzes, it was hypothesized that the amount of the water loss was negligible with almost no change in the electrolyte concentration.

To demonstrate the feasibility of using the HEA cyclic electroplating for the development of wearable electronics, conductive templates were applied on a piece of Laminated Polyester Ripstop (purchased from Rockywoods Fabrics) substrate using in-house made carbon nanotube (CNT) ink. The CNT ink was synthesized as explained in our earlier works [17–19] by adding 300 mg of multiwalled CNTs (from Sigma) and 150 mg of sodium dodecylbenzenesulfonate (SDBS) into 30 mL of DI water and sonicated to obtain a homogenous mixture. Conductive patterns in form of tracks (strips with a width of  $\sim 3$  mm and length of 1.5 cm) were applied on the fabric using kapton tape as a mask and the CNT solution as the ink. A similar setup as shown in Fig. 1.a was used for electroplating the conductive patterns on the fabric substrate. However, instead of wires connected to the cathodes, connections to the conductive patterns were made by hand sewing Jameco conductive thread. At last, superglue was used to glue a surface mount red LED (Oznum 3528) to the fabric next to the CNT tracks.

## 3. Results and discussion

Fig. 1b shows the patterned copper tracks on PCB with the 1 mm gap that were used as the cathodes. Fig. 1c and d show the images of the sample during and after the HEA electrodeposition, respectively. The hydrogen bubbles are visible in Fig. 1c. Also, Fig. 1d shows bridging the gap between the two cathodes after the electroplating.

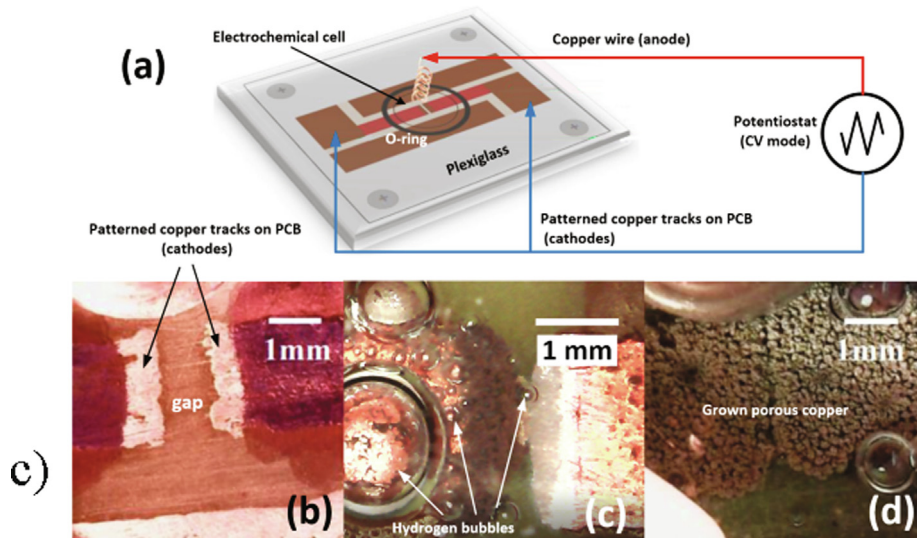


**Fig. 1.** a) Schematic of the electrochemical cell with the cathodes being patterned on a PCB with a copper wire as the anode and an O-ring holding the electrolyte. A sawtooth shape voltage was applied to the cell through a potentiostat under the CV mode. Images of the cathodes (b) before, (c) during, and (d) after the HEA electroplating.

Fig. 2 shows the second loop of the CV results for seven samples that were tested for a voltage range between  $-0.8$  V and  $-1.3$  V at different scan rates. The number of cycles was different in different experiments based on the speed of growing copper across the gap. At very low scan rates (i.e.,  $5$  mV/s and  $10$  mV/s), the situation was similar to the constant voltage growth condition reported in our previous work [9]. In that case, the generated hydrogen bubbles almost blocked the surface of the cathodes and limited the access of the  $\text{Cu}^{2+}$  to the electrodes for further electrodeposition. Because of that, the current level was almost constant at  $-60$  mA for  $5$  mV/s and  $-80$  mA for  $10$  mV/s. It was observed that when faster scan rates were applied, the CV loops presented two distinct sections. The first section, closer to  $-0.8$  V, was without hydrogen evolution that showed smooth curves with a shallow slope of the current. However, the second part of each curve closer to  $-1.3$  V occurred when the hydrogen bubbles were released as the copper was growing. The effect of hydrogen evolution was to enhance the copper growth which resulted in a sharper slope in the current. Also, the disturbance due to the hydrogen bubbling generated a relatively large ripple in the current as the voltage was scanned. Exceptions are at very fast scan rates of  $300$  mV/s and  $500$  mV/s in which scanning the voltage back and forth between  $-0.8$  V and  $-1.3$  V took only a few seconds with almost no ripple in the current. Similar features as presented in Fig. 2 were observed in the CV results when samples were tested under different voltage ranges of  $-1.5$  V  $\leq V \leq -0.8$  V,  $-1.3$  V  $\leq V \leq -1.0$  V, and  $-1.5$  V  $\leq V \leq -1.0$  V. Considering that the grown copper is a continuous structure of metal with the conductivity of pure copper ( $\sim 0.6 \times 10^6$  S/cm), the two-probe resistance test between the two cathodes showed  $0.0 \Omega$  across the gaps after being bridged through the electroplating process.

To find the correlation between the voltage ranges and the lateral growth rates, the growth rate for each sample was estimated from the time that it took for the copper to bridge the gap and was plotted versus the scan rate for four different voltage ranges in Fig. 3. The results clearly show that the growth rate is very slow at low scan rates, regardless of the voltage range. By increasing the scan rate, almost the fastest growth rate was achieved when the scan rate was at  $50$  or  $100$  mV/s, except for the voltage range 'd', in which the fastest rate occurred at  $300$  mV/s. An interesting aspect of the results is the decrease in the growth rate at higher scan rates. Among all different growth conditions, the fastest rate of  $55 \mu\text{m/s}$  was achieved in the voltage range 'b' ( $V_{\text{max}} = -0.8$  V and  $V_{\text{min}} = -1.5$  V) at  $100$  mV/s. Such a speed is not only the highest among all of the samples in this study, but

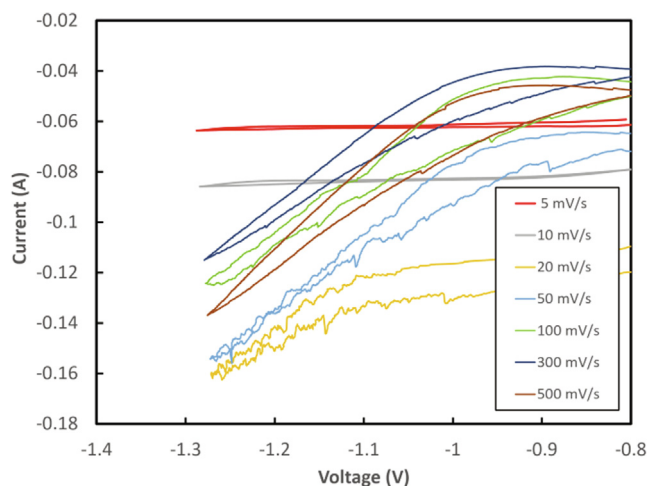


Fig. 2. CV results for the samples grown between  $-0.8$  V and  $-1.3$  V (voltage range 'a') at different scan rates. Only the second cycles are presented.

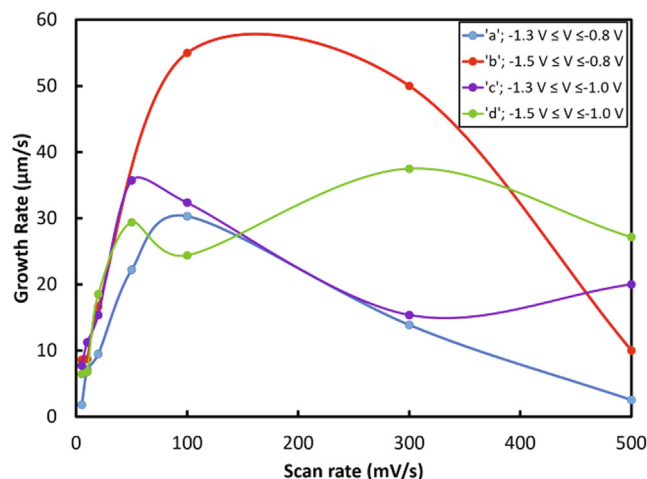
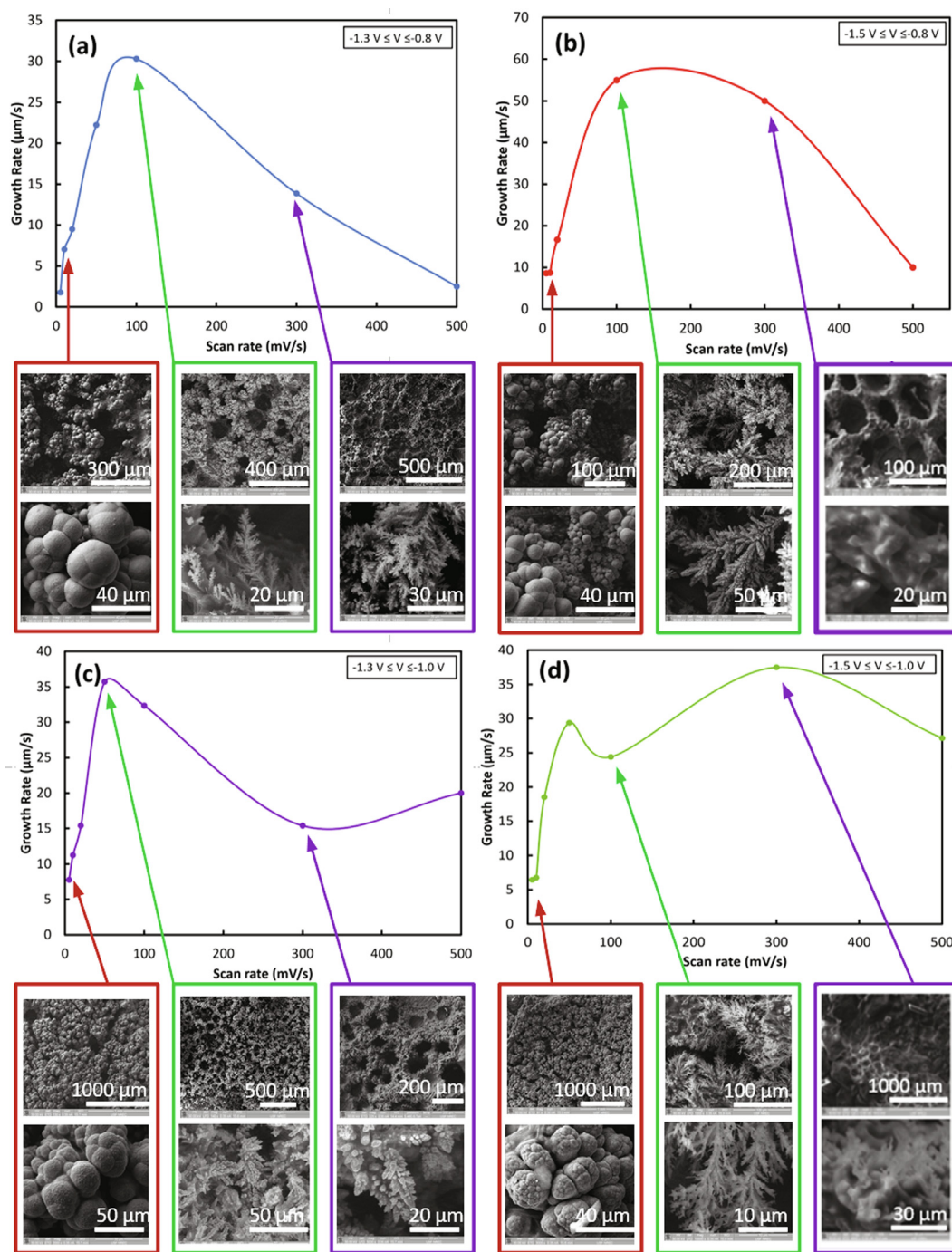


Fig. 3. Copper lateral growth rate vs. voltage scan rate for four different voltage ranges.

also  $3.5 \times$  higher than the growth speed in our earlier work when  $-1.3$  V DC was applied to the cathode [10].

To understand the effect of the growth conditions on the quality of the grown copper layer, SEM images were taken from different samples. Fig. 4 shows the images of the samples at low, high, and mid scan rates for each voltage range. It is found that, in all of them, at low scan rates, the deposited copper had a relatively compact and cauliflower-like structure with micron-size spherical shapes. Similar microstructures were observed when only DC voltage was used for HEA copper electroplating [9]. As shown in the images, near  $100$  mV/s, the micro-spheres were disappeared, and instead, dendrites were formed developing structures in form of ferns. Also, the porous structure of copper was evident. At higher scan rates, the nice fern-shape structures were almost deformed to shape a honeycomb structure at the submillimeter scale. Considering that the amount of copper needed for making a highly porous structure can be substantially lower than a denser structure, achieving the fastest growth rate around  $100$  mV/s can be explained by the produced highly porous structure around that scan rate. Another noticeable feature was the size of the pores in different curves around  $100$  mV/s. Among all, the largest pores of  $\sim 200 \mu\text{m}$  were formed in the voltage range 'b' at the fastest growth rate of  $55 \mu\text{m/s}$ . The average pore size in 'a', 'c', and 'd', were  $\sim 100 \mu\text{m}$ ,  $\sim 50 \mu\text{m}$ , and  $\sim 50 \mu\text{m}$ , respectively. The large pores in 'b' resulted in a lower density of the porous copper layer which consequently can grow faster than layers with the smaller pores. Regarding the reason why the nanostructures are different at different scan rates, more in-depth studies are required to better understand the concurrent reduction of  $\text{Cu}^{2+}$  and  $\text{H}^+$  at the cathode in the HEA mode.

Analyzing the electrochemical current in a HEA process is very complicated because a part of the cathodic current is consumed for the generation of hydrogen and the rest participates in the reduction of the  $\text{Cu}^{2+}$  ions at the cathodes. Potentially, the rate of the released hydrogen can be measured accurately to estimate the average rate of the deposited copper in each of the HEA experiments. However, such a study requires a different electrochemical cell design for the efficient collection of the released hydrogen gas. Therefore, here, we have analyzed the process only based on the voltage range and the scan rate. To comprehend the difference in the growth processes in different cases, in Fig. 5, the voltage variations vs. time are plotted for all four voltage ranges. Since water electrolysis at  $1.23$  V, the  $-1.23$  V level is shown in the plots as the boundary for starting the hydrogen evolution near the cathodes. It should be noted that, in practice, the transition between HEA and non-HEA modes is not a binary transition, but the electrolysis rate increases exponentially as the voltage gets closer to



**Fig. 4.** Selected SEM images of different samples associated to their growth conditions. Two SEM images with different zooming scales are presented for each sample.

– 1.23 V and strong electrolysis is expected beyond – 1.23 V. Hence, in Fig. 5, the part of the voltage in each cycle with a value less than – 1.23 V is marked with a shaded triangle, indicating the expected HEA electroplating. As shown in Fig. 5, the cyclic method is actually a triangle waveshape AC voltage with an amplitude of  $V_{AC} = |V_{max} - V_{min}|/2$  being superimposed to a DC voltage of  $V_{DC} = (V_{max} + V_{min})/2$ .

Fig. 5a shows that, regardless of the scan rate, HEA covers a small fraction of each cycle. Also, a relatively large voltage difference between  $V_{DC} = -1.05$  V and – 1.23 V explains why even at the fastest growth rate, the growth speed was limited to 30.3  $\mu\text{m/s}$ . Although similar to the voltage range ‘c’ (Fig. 5c), the shaded area shows a small fraction of each cycle,  $V_{DC} = -1.15$  V is closer to – 1.23 V than that

in ‘a’. This may explain a slightly higher speed of 35.7  $\mu\text{m/s}$  at 50 mV/s compares to the fastest case in ‘a’. As shown in Fig. 5b, a much larger portion of each cycle covers the HEA mode with  $V_{DC}$  of – 1.15 V. This can be the reason for achieving 55  $\mu\text{m/s}$  and 50  $\mu\text{m/s}$  at 100 mV/s and 300 mV/s, respectively. Fig. 5d shows that due to  $V_{DC}$  of – 1.25 V (being less than – 1.23 V), more than 50% of each cycle is in the HEA mode. However, the growth rate in ‘d’ never exceeded 37.5  $\mu\text{m/s}$ . This is likely due to the lack of enough time in each cycle for releasing the hydrogen bubbles. Hence, similar to the limitations with the constant voltage experiments [10], the blockage of the electrode area with the stuck bubbles has limited the growth rate. In fact, the morphology of

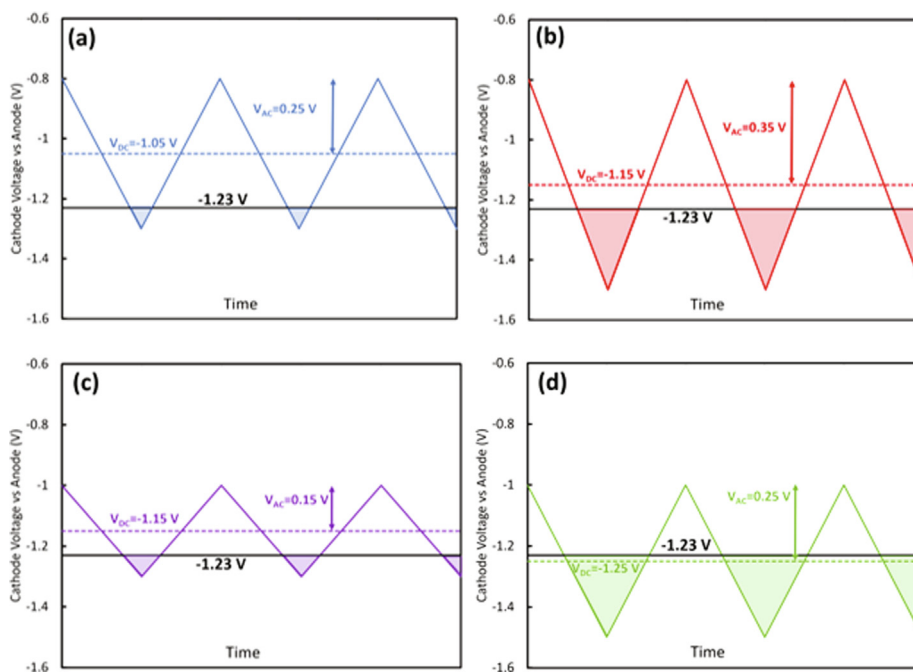


**Fig. 5.** The voltage variation in the voltage ranges of ‘a’, ‘b’, ‘c’, and ‘d’. The shaded area on each curve shows the portion of each cycle at which the voltage of the cell exceeded the value required for the water electrolysis with strong HEA copper deposition. Although water electrolysis starts even before the voltage reaches  $-1.23$  V, the  $-1.23$  V voltage level is marked in all the plots as a reference level to compare different cases.

the samples through the SEM images shows a larger variation in the pore sizes as evidence of the agglomeration of the hydrogen bubbles.

While the voltage profiles explain why ‘b’ is preferred, for a better understanding of the scan rate effect, we should consider the period of each cycle. As explained, low scan rates of 5 to 20 mV/s are more like DC cases with an extended period of time staying in the HEA and non-HEA modes. At higher scan rates near to 500 mV/s, it takes only a few seconds for the voltage to switch back and forth between the HEA and non-HEA modes. Hence, the effect of switching between the two modes is not fully reflected in the results. Apparently, a scan rate of 100 mV/s is the best for achieving the fastest growth in cases ‘b’. Considering the voltage range of  $-1.5$  V to  $-0.8$  V, 100 mV/s corresponds to the period of  $T = 14$  s. Since a portion of each cycle is dedicated to the HEA mode, the results suggest that after a few seconds of HEA copper growth, it is better to conduct the growth in a non-HEA mode for a few seconds to allow the generated bubbles to leave the surface before their agglomeration.

Following the successful cyclic electroplating method on PCBs for the voltage range of  $-1.5$  V  $\leq$  V  $\leq$   $-0.8$  V and scan rate of 100 mV/s, an experiment was designed to apply the HEA method for growing copper on fabrics for developing wearable electronics. As shown in Fig. 6a, first, using the CNT ink, a conductive pattern in form of two strips was applied on a piece of Laminated Polyester Ripstop fabric. The choice of the fabric was based on our earlier studies [17]. The surface resistance of the conductive part after coating was measured with the four-point method and found to be  $R_{s-\text{ink}} = 30\text{--}60$   $\Omega/\square$ . A surface mount LED was glued to the fabric between the two strips while there was a sub-millimeter gap between the device terminals and the edge of the strips (Fig. 6b). A setup like the one shown in Fig. 1a was used to grow copper on the CNT ink and across the gap between the tracks and LED. Fig. 6c shows the hydrogen bubbles during the HEA mode. During the experiment, first, a copper layer grew over the CNT ink pattern. Then, the copper grew across the gap to ‘solder’ (electrochemical soldering) the device terminals to the tracks. Fig. 6d shows the sample after the electroplating process when the electrolyte was removed from the cell. Jameco conductive thread that was sewed to the conduc-

tive pattern (outside the O-ring) and used as the wire for connecting to the potentiostat is shown in that figure. The part of the conductive strips that was inside the electrochemical cell (inside the O-ring area) was coated with a uniform but the porous structure of copper. The electroplated nanostructure was well diffused into the fabric structure and resulted in a mechanically robust metal coating. Yet, the fabric flexibility was maintained without any noticeable change in the copper layer after bending the fabric. The resistance of the metal-coated part was measured again after the copper electroplating and it was found to be  $R_{s-\text{Cu}} = 7$  m $\Omega/\square$  (four orders of magnitude more conductive than before the electroplating). Such low resistance confirms that the cyclic HEA electroplating can be used for the deposition of copper on fabrics to apply an electronic circuit layout. In fact, the conductivity of the electroplated copper is the same as that for a copper layer on a PCB and 200  $\times$  better than the conductivity of the inkjet-printed metal nanoparticles used for wearable electronics [20]. As the zoomed picture in Fig. 6e shows, the copper layer also made a solid joint to the terminal of the LED and practically soldered the component to the tracks. The electrical contact between the track and the LED was verified by powering the LED through an external power source. As shown in Fig. 6f, light was emitted from LED when it was powered. To investigate the adhesion of the copper layer to the fabric substrate, we applied the basic adhesion test using a piece of Scotch tape. Fig. 6g shows the zoomed-in image of the copper layer before the adhesion test. A piece of tape was applied and pressed gently on the copper layer. After peeling off the tape another optical image was taken from the area. As shown in Fig. 6h, no noticeable change in the morphology was observed. Also, the electrical resistance of the copper layer before and after the adhesion test was measured to be 0.0  $\Omega$ , using the two-probe method. Both the optical images and the resistance test verified the good adhesion of the grown copper to the fabric structure, most likely due to the anchoring of the copper nanostructure to the fibers of the fabric. The experiments on the fabric verify the feasibility of using the cyclic HEA electroplating for both applying a metallic pattern on the fabric and soldering components to the circuit layout. Considering that the cyclic HEA method was conducted at room

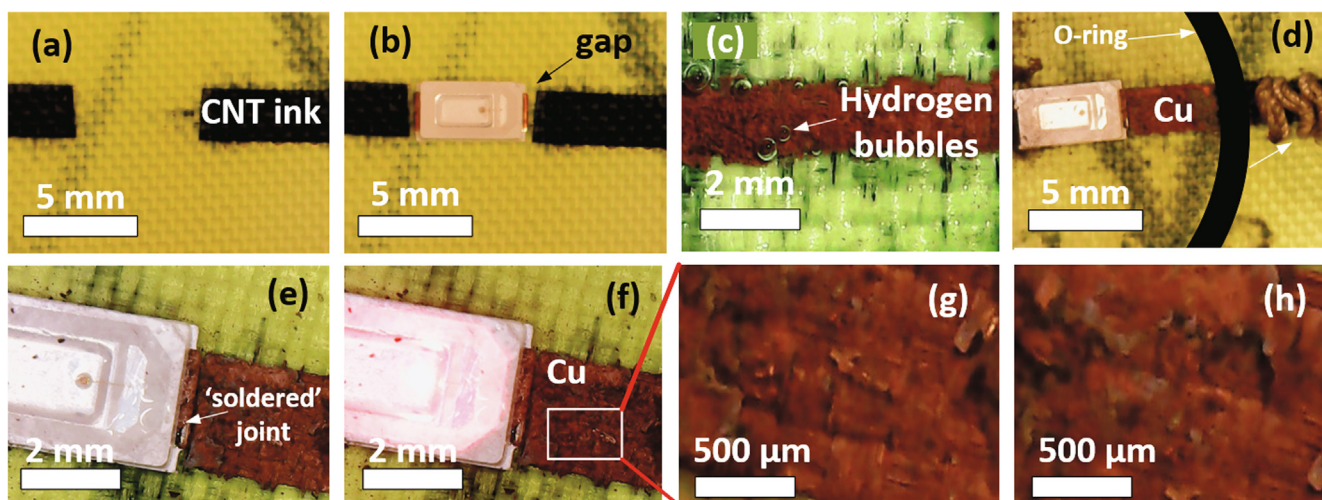


**Fig. 6.** Optical images of the experiment showing the steps in applying the cyclic HEA method for the development of wearable electronics and testing the functionality of an LED being soldered via the electroplating method. The conductive pattern on a piece of fabric (a) before and (b) after gluing the LED. Pictures of the sample (c) during and (d) after the electroplating. The joint between the LED terminal and the electroplated track (e) before and (f) during powering the LED. Zoomed-in images of the grown copper (g) before and (h) after the adhesion test.

temperature, this soldering method is more suitable than the conventional soldering method using soldering irons that can damage fabric substrates. Also, the experiment verifies that despite soaking the LED into the electrolyte during the electroplating, there is no damage to the electronic components. Further experiments are planned to study the effect of the cyclic HEA electroplating on the mechanical stability of the copper coating on different fabrics. Also, to apply the method for developing practical wearable electronics, we are planning to study the effect of a passive coating layer over copper to be able to wash the fabric without damaging the circuit.

#### 4. Conclusions

Employing the cyclic HEA method, copper was successfully grown across a non-conductive gap by the application of a superimposed triangle wavelike AC voltage to a DC voltage in a localized electrochemical cell. The applied alternative voltage resulted in an alternation between the HEA and non-HEA electroplating modes through which the generated hydrogen bubbles had time to leave the surface which resulted in more uniform copper growth. The results showed that the fastest growth for copper electrodeposition was achieved at a scan rate of 100 mV/s when the voltage of the cell was limited between  $-1.5$  V and  $-0.8$  V. Also, it was found that the portion of each cycle that is in the HEA mode has a direct impact on the nanostructure of the grown copper. The cyclic HEA method was then tested for growing copper over a piece of fabric and electrochemically soldering of an LED to the conductive pattern on the fabric. Further study on adapting the process for the development of wearable electronics is recommended for future works.

#### Declaration of Competing Interest

The authors declare that they have no known competing financial interests or personal relationships that could have appeared to influence the work reported in this paper.

#### Acknowledgement

This work was supported by the National Science Foundation through NSF 1953089 and NASA FSGC-15 05 award.

#### References

- [1] D. Gabe, A. Cobley, Catalytic anodes for electrodeposition: a study for acid copper printed circuit board (PCB) production, *Circuit World* (2006).
- [2] L. Yin, Z. Liu, Z. Yang, Z. Wang, S. Shingubara, Effect of PEG molecular weight on bottom-up filling of copper electrodeposition for PCB interconnects, *Transactions of the IMF* 88 (2010) 149–153.
- [3] Y.F. Guimarães, I.D. Santos, A.J. Dutra, Direct recovery of copper from printed circuit boards (PCBs) powder concentrate by a simultaneous electroleaching–electrodeposition process, *Hydrometallurgy* 149 (2014) 63–70.
- [4] J.G. Kaufmann, M.P. Desmulliez, Y. Tian, D. Price, M. Hughes, N. Strusevich, C. Bailey, C. Liu, D. Hutt, Megasonic agitation for enhanced electrodeposition of copper, *Microsystem technologies* 15 (2009) 1245–1254.
- [5] S. Costello, N. Strusevich, D. Flynn, R.W. Kay, M.K. Patel, C. Bailey, D. Price, M. Bennet, A.C. Jones, M.P.Y. Desmulliez, Electrodeposition of copper into high aspect ratio PCB micro-via using megasonic agitation, *Microsystem technologies* 19 (2013) 783–790.
- [6] E. Vaněčková, M. Bouša, R. Sokolová, P. Moreno-García, P. Broekmann, V. Shestivska, J. Rathouský, M. Gál, T. Sebechlebská, V. Kolivoška, Copper electroplating of 3D printed composite electrodes, *Journal of Electroanalytical Chemistry* 858 (2020) 113763, <https://doi.org/10.1016/j.jelechem.2019.113763>.
- [7] A.J. Cobley, D.R. Gabe, Characterisation of insoluble anodes for acid copper electrodeposition, *Transactions of the IMF* 81 (2) (2003) 37–44.
- [8] A.J. Bard, L.R. Faulkner, J. Leddy, C.G. Zoski, *Electrochemical methods: fundamentals and applications*, Wiley New York, 1980.
- [9] S.M. Rosa-Ortiz, K.K. Kadari, A. Takshi, Low Temperature Soldering Surface-Mount Electronic Components with Hydrogen Assisted Copper Electroplating, *MRS Advances* 3 (18) (2018) 963–968.
- [10] S.M. Rosa-Ortiz, F. Khorramshahi, A. Takshi, Study the impact of CuSO 4 and H 2 SO 4 concentrations on lateral growth of hydrogen evolution assisted copper electroplating, *Journal of Applied Electrochemistry* 49 (12) (2019) 1203–1210.
- [11] N. Nikolić, G. Branković, M. Pavlović, K. Popov, The effect of hydrogen codeposition on the morphology of copper electrodeposits. II. Correlation between the properties of electrolytic solutions and the quantity of evolved hydrogen, *Journal of Electroanalytical Chemistry* 621 (2008) 13–21.
- [12] N. Nikolić, K. Popov, L.J. Pavlović, M. Pavlović, Phenomenology of a formation of a honeycomb-like structure during copper electrodeposition, *Journal of Solid State Electrochemistry* 11 (2007) 667–675.
- [13] N. Nikolić, K. Popov, L.J. Pavlović, M. Pavlović, The effect of hydrogen codeposition on the morphology of copper electrodeposits. I. The concept of effective overpotential, *Journal of Electroanalytical Chemistry* 588 (2006) 88–98.
- [14] N. Nikolić, K. Popov, L.J. Pavlović, M. Pavlović, Morphologies of copper deposits obtained by the electrodeposition at high overpotentials, *Surface and Coatings Technology* 201 (2006) 560–566.
- [15] S.M. Rosa-Ortiz, A. Takshi, S. Thomas, Advances in lateral copper electroplated metallic tracks—production and applications by using hydrogen evolution-assisted electroplating, *MRS Advances* 6 (26) (2021) 654–658.
- [16] H.-C. Shin, J. Dong, M. Liu, Nanoporous structures prepared by an electrochemical deposition process, *Advanced Materials* 15 (19) (2003) 1610–1614.
- [17] S.M. Rosa-Ortiz, A. Takshi, Copper Electrodeposition by Hydrogen Evolution Assisted Electroplating (HEA) for Wearable Electronics, 2020 Pan Pacific Microelectronics Symposium (Pan Pacific), IEEE 2020 (2020) 1–5.
- [18] Belqasem Aljafari, Sharan K. Indrakar, Manoj K. Ram, Prasanta K. Biswas, Elias Stefanakos, Arash Takshi, A Polyaniline-Based Redox-Active Composite Gel

- Electrolyte with Photo-Electric and Electrochromic Properties, *ChemElectroChem* 6 (23) (2019) 5888–5895.
- [19] Belqasem Aljafari, Turki Alamro, Manoj K. Ram, Arash Takshi, Polyvinyl alcohol-acid redox active gel electrolytes for electrical double-layer capacitor devices, *Journal of Solid State Electrochemistry* 23 (1) (2019) 125–133.
- [20] Bauyrzhan Krykpayev, Muhammad Fahad Farooqui, Rana Muhammad Bilal, Mohammad Vaseem, Atif Shamim, A wearable tracking device inkjet-printed on textile, *Microelectronics Journal* 65 (2017) 40–48.